Strain localization in polyurethane foams. Experiments and theoretical model.

Giampiero Pampolini, Gianpietro del Piero

Noname manuscript No.
(will be inserted by the editor)

Strain localization in polyurethane foams. Experiments and theoretical model.

Giampiero Pampolini · Gianpietro Del Piero

Received: date / Accepted: date

Abstract Strain localization has been observed in polyurethane foams subjected to confined compression up to 70% of deformation. This phenomenon is described by a one-dimensional model, in which the foam is represented as a chain of non-linear elastic springs with non-convex strain energy density, and localization is attributed to progressive phase transition.

Keywords polyurethane foams · strain localization · non-convex strain energy, solid-solid phase transition.

1 Introduction

In the uniaxial compression of foam polymers, and of cellular materials in general, three regimes can be identified. The first regime is an almost linear response, the second is a stress plateau with large displacements occurring at almost constant load, and the last is a branch characterized by large stress increase under relatively moderate deformations. In the literature, two main approaches for modeling the mechanical response of foam polymers are used: a microstructural approach, reproducing directly the microstructure with a complex structure of beams, and a macroscopic approach, based on a full three-dimensional representation of the material as a continuum. There has been a wide spread of models based on the first approach (e.g., [Gent and Thomas (1963)], [Gibson and Ashby (1997)], [Warren and Kraynik (1997)], [Gong et al. (2005)]). In particular, Gong et al. studied the response curves of open-cell foams, and [Gong and Kyriakides (2005)] proposed a model with a periodic struc-

Giampiero Pampolini
Laboratoire de Mécanique et d'Acoustique, CNRS, 31 chemin Joseph Aiguier, 13402 Marseille, France.
Università di Ferrara, Via Saragat 1, 44100 Ferrara, Italy.
E-mail: pampolini@lma.cnrs-mrs.fr; giampiero.pampolini@unife.it

Gianpietro Del Piero
Università di Ferrara, Via Saragat 1, 44100 Ferrara, Italy.
E-mail: dlpgpt@unife.it

ture given by a 14-sided polyhedron, called the Kelvin cell. The ligaments are modeled as shear-deformable extensional beams, and the basic material is assumed to be linearly elastic. In this approach, the numerical simulation is demanding from the computational point of view, due to the complexity of the assumed microstructure and to the difficulty of modeling the contact between beams in the post-buckling regime, see [Bardenhagen et al. (2005)]. In the continuum approach, the material is considered as homogeneous and hyperelastic, and subject to non-homogeneous deformations. Indeed, there is experimental evidence of strain localization, see for example [Lakes et al. (1993)], [Wang and Cuitinho (2002)]. In particular, strain localization along bands orthogonal to the loading direction was observed by Wang and Cuitio, and confirmed by experiments performed by the present authors on polyurethane foam specimens, subjected to axial compression up to 70%. The same three stages in the evolution of deformation have been observed by [Bastawros et al. (2000)] and [Bart-Smith et al. (1998)] in both open- and closed-cell aluminium alloy foams. In these cases, the deformation localizes in narrow bands, whose width is of the order of a cell diameter. These results support the interpretation, suggested in previous works [Wang and Cuitinho (2002)], [Gioia et al. (2001)], of the non-homogeneous deformation as a phase transition. Here we present a model in which the foam is represented as a chain of non-linear elastic springs with non-convex strain energy, and the localization is interpreted as a progressive phase change. The first part of the paper deals with the test procedure and the experimental results, and the second contains an outline of the theoretical model. A complete description of the model can be found in [Pampolini and Del Piero (2008)].

2 EXPERIMENTAL TESTS

For the compression tests we used the load frame INSTRON 4467 located at the *Laboratorio di Materiali Polimerici* of the University of Ferrara, with a load cell of 500 N. The tests were made on commercial polyurethane foams in confined compression. For confinement we used a polystyrene box, clamped to the load frame. The polystyrene box is more rigid than the tested material and, being transparent, allowed us to control optically the evolution of the deformation. At the upper basis, the specimen was in contact with a steel plate fixed to the moving crosshead. Five specimens of dimensions 100 $\times$ 100 $\times$ 50 mm were tested. The crosshead speed was chosen to be 1 mm/min, which we believe small enough to neglect all rate-dependent effects. The test was stopped at a relative elongation of 70%. As we will see later, this value is sufficiently large to include the significant portions of the response curves.

The stress-strain curves shown in Figure 1 reveal the characteristic behavior of polyurethane foams, and of cellular materials in general. From the figure, we notice that the plateau begins at a relative elongation of about 10% and ends at about 63%, and that the stress is close to 6,5 kPa. The slope of the second branch is approximatively 25 kPa. These values are close to those obtained by [Gioia et al. (2001)].

During the tests, the deformation was initially homogeneous (Figure 2a). Then a severe deformation occurred at the upper layer of the specimen (Figure 2b), and propagated to the underlying layers (Figures 2c, 2d). When all layers had reached the same deformation the specimen began again to deform homogeneously (Figure 2e). That the large deformation regime starts at one of the ends of the specimen can be attributed to a local boundary effect due to contact between steel plate and specimen. The same

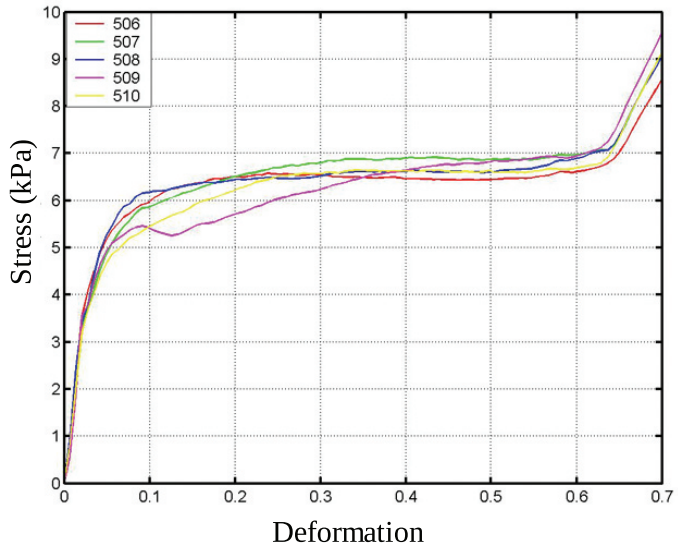

Fig. 1 Experimental curves of polyurethane foams in confined compression tests.

evolution mechanism was observed by [Wang and Cuitinho (2002)] in polyurethane low-density foams, and by [Bastawros et al. (2000)] and [Bart-Smith et al. (1998)] in aluminium alloy foams. In Wang and Cuitio's experiments, localization does not initiate at the upper part of the specimen as it does in our tests.

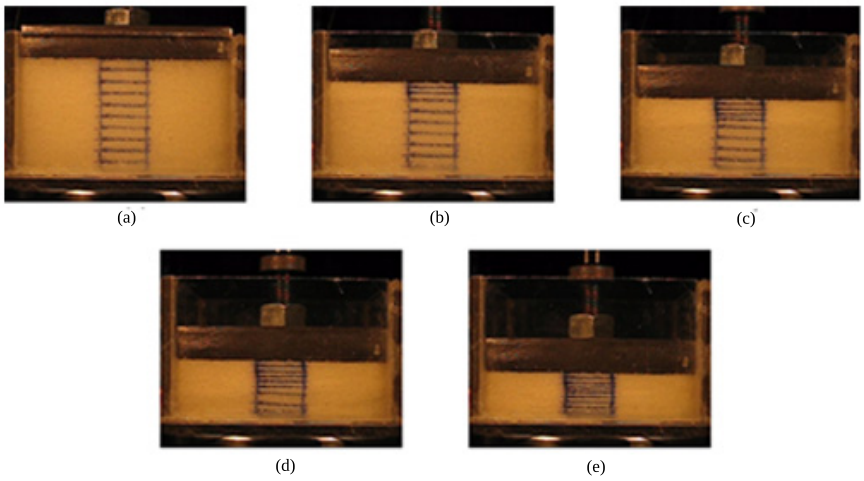

Fig. 2 Progressive deformation mechanism. Initial homogeneous deformation (a). Strain localization at the upper end of the specimen (b). Propagation to the underlying layers (c), (d). Back to homogeneous deformation (e).

3 THE THEORETICAL MODEL

3.1 Constitutive assumptions

Let Ω_0 be the bounded open region of the three-dimensional space occupied by the body in the reference configuration, and let f be the deformation that maps the points X of Ω_0 into the points $x = f(X)$. Denote by Ω the region $f(\Omega_0)$ occupied by the deformed body, and by F the deformation gradient ∇f. Assume that the body is made of an isotropic hyperelastic material, with a strain energy density of the form

$$w(F) = \frac{1}{2}\alpha\, F \cdot F + \Gamma\left(\det F\right). \tag{1}$$

where α is a positive material constant, and Γ is a function which takes the value $+\infty$ for both $\det F = 0$ and $\det F = +\infty$

$$\lim_{\det F \to 0} \Gamma\left(\det F\right) = \lim_{\det F \to \infty} \Gamma\left(\det F\right) = +\infty. \tag{2}$$

The gradient of w

$$S = w_F\left(F\right) = \alpha F + \det F\, \Gamma'\left(\det F\right) F^{-T}, \tag{3}$$

is the Piola-Kirchhoff stress tensor. If we impose that the reference configuration $F = I$ be stress-free, from the conditions $w(I) = w_F(I) = 0$ we get

$$\alpha = -\Gamma'(1), \quad \frac{3}{2}\alpha + \Gamma(1) = 0. \tag{4}$$

For the function Γ we assume the expression

$$\Gamma\left(\det F\right) = c\left(\det F\right)^n \left(\frac{1}{n+2}\left(\det F\right)^2 - \frac{1}{n}\right) - \mu \ln\left(\det F\right) + \frac{1}{2}\frac{\beta\sqrt{\pi}}{\sqrt{k}} \operatorname{erf}\left(\sqrt{k}\left(\det F - a\right)\right) + \gamma, \tag{5}$$

where $\alpha, c, n, \mu, \beta, k$ are positive constants, with $a \leq 1$, $\operatorname{erf}(\cdot)$ is the error function

$$\operatorname{erf}(x) = \int_0^x \frac{2}{\sqrt{\pi}} e^{-t^2}, \tag{6}$$

and γ is the constant determined by the condition $3\Gamma'(1) = 2\Gamma(1)$. The expression (5) of Γ consists of two parts. The first part is similar to that one proposed in [Ogden (1997)], and takes into account the long-range effects. The second part, the error function, provides a local effect at values of $\det F$ close to a. In the particular case of confined compression in the direction e, one has $F = I + (\lambda - 1)e \otimes e$. Then , for Γ as in (5), the energy density is

$$w(\lambda) = \frac{1}{2}\alpha\left(2 + \lambda^2\right) + \Gamma(\lambda), \tag{7}$$

and the normal component of S in the direction of loading is

$$\sigma = \left[\mu - \beta \exp\left(-k(1-a)^2\right)\right]\lambda + c\lambda^{n-1}\left(\lambda^2 - 1\right) - \mu\lambda^{-1} + \beta \exp\left(-k(\lambda - a)^2\right). \tag{8}$$

The energy has the non-convex form shown in Figure 3c, and the stress-strain curve has two ascending branches separated by a descending branch, as shown in Figure 3d.

3.2 The discrete model

Consider a chain of n springs connected in series as sketched in Figure 3a, each spring representing a layer of cells as shown in Figure 3b. We assume that all springs have the same strain energy w given by (7), and that, accordingly, the stress-strain curve is given by (8). The total energy of the system is the sum of the strain energies of the springs,

$$E\left(\varepsilon_1, \varepsilon_2, ..., \varepsilon_n\right) = \sum_{i=1}^{n} w(\varepsilon_i), \tag{9}$$

where ε_i is the elongation of the i-th spring. The bar is subjected to the *hard device* condition

$$\sum_{i=1}^{n} \varepsilon_i = n\varepsilon_0, \tag{10}$$

where $n\varepsilon_0$ is the imposed displacement at the upper basis, the displacement at the lower basis being zero. By setting to zero the partial derivatives of the total energy, one gets the equilibrium condition

$$w'\left(\varepsilon_i\right) = w'\left(\varepsilon_n\right), \qquad i = 1, 2, ..., n-1. \tag{11}$$

which implies that the force is the same in all springs. The common value of the force will be denoted by σ.

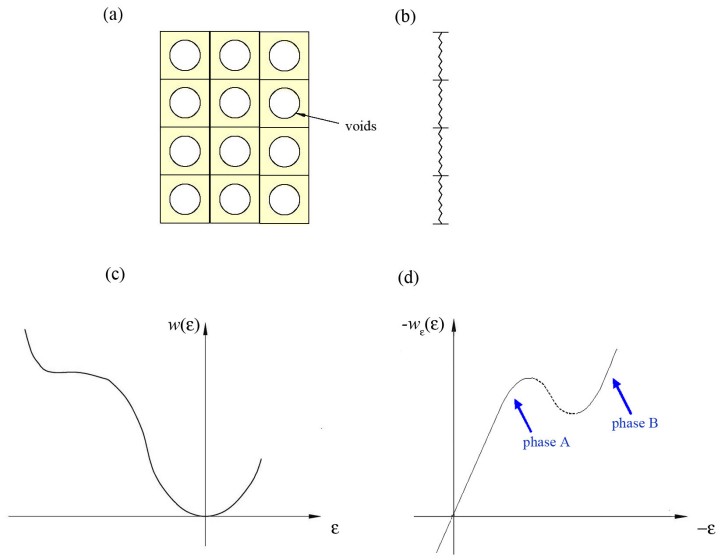

Fig. 3 Subdivision of the body into cell layers (a), representation of each layer as a non linear elastic spring (b) with non convex energy (c), and non-monotonic stress-strain curve (d).

For sufficiently large n, a sufficient condition for stability is that all elongations ε_i lie on an ascending branch of the stress-strain curve, see [Del Piero and Truskinowsky (2008)] or [Puglisi and Truskinovsky (2000)]. Therefore, we confine our attention to the equilibrium configurations which satisfy this condition. For every such configuration, let m be the number of the springs whose elongations lie on the first ascending branch (phase A), so that $(n-m)$ is the number of the springs whose elongations lie on the second ascending branch (phase B). In particular, for $m=0$ and for $m=n$ we have single-phase configurations, and for $0<m<n$ we have two-phase configurations. In a single-phase configuration, all springs have the same elongation

$$\varepsilon_0 = \varepsilon_i, \qquad i = 1, 2, ..., n, \tag{12}$$

and the global response curve (σ, ε_0) coincides with the response curve (σ, ε_i) of each spring. In a two-phase configuration, let $\bar{\sigma}$ be the force in the springs, and let $\bar{\varepsilon}_1$ and $\bar{\varepsilon}_2$ be the elongations corresponding to $\bar{\sigma}$ in the first and second ascending branch, respectively. Then the total elongation of the chain is

$$n\bar{\varepsilon}_0 = m\bar{\varepsilon}_1 + (n-m)\bar{\varepsilon}_2. \tag{13}$$

By varying $\bar{\sigma}$, one can construct the equilibrium path $(\bar{\sigma}, \bar{\varepsilon}_0)$ corresponding to each given m. By dividing the interval $(\bar{\varepsilon}_1, \bar{\varepsilon}_2)$, into n equal parts, all equilibrium paths for different m are obtained. In Figure 4a, these paths are shown for a system of 4 springs.

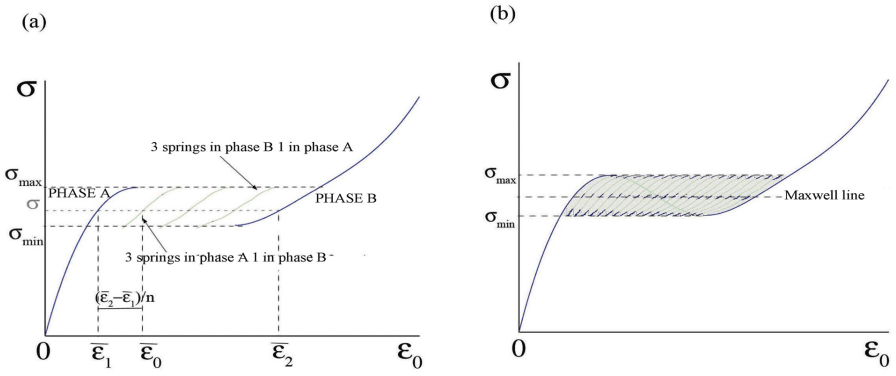

Fig. 4 Response curves for a system of 4 springs (a) and for a system of 20 springs (b).

If one assumes that the system evolves along equilibrium curves made of local energy minimizers, then the system, when loaded starting from the initial configuration, initially follows the first ascending branch. This branch ends when the stress reaches the critical value σ_{max} shown in Figure 4a. At this point, for further increasing deformation it is reasonable to assume that the system jumps to the closest stable branch, corresponding to the configuration with one spring in phase B and three springs in phase A. When this branch ends, the system jumps to the branch with two springs in phase B and so on, until all springs undergo the phase transition. At this point the system evolves following the second ascending branch, which corresponds to single-phase configurations with all springs in phase B. If we now increase the number of springs

(Figure 4b), the number of the intermediate branches increases, and the amplitudes of the jumps at the end of the branches decrease. In this case when the stress reaches the critical value σ_{max}, the system follows a wavy, approximately horizontal line, successively assuming configurations with p springs in the highly deformed phase B and $n-p$ springs in the low-deformation phase A, with p gradually increasing from zero to n. At unloading the system exhibits a similar behavior, after reaching the critical stress σ_{min}. The model therefore predicts a hysteresis loop, which has indeed been observed experimentally [Gong and Kyriakides (2005)].

3.3 Comparison with the experimental data

In Figure 5 the model response is compared with the experimental results. The dotted line is the average loading curve, obtained as an average of the experimental curves shown in Figure 2. The solid line is the response curve of the model for a system of a sufficiently large number of springs with strain energy of the type (1), evaluated with the constitutive data reported in Table 1.

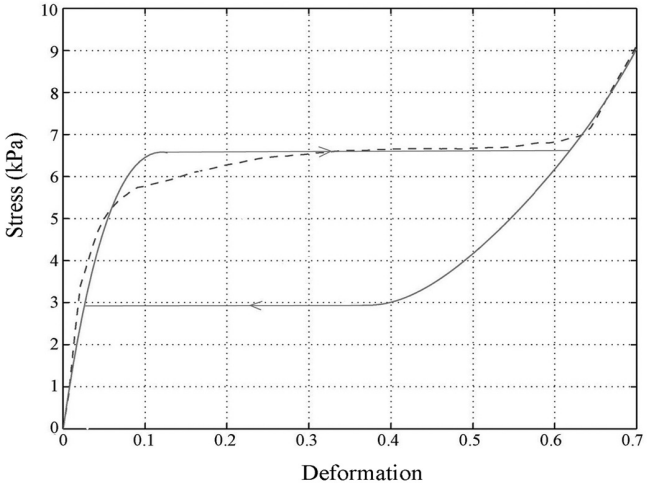

Fig. 5 Theoretical response curves and hysteresis loop at loading and unloading (solid lines), compared with experimental response at loading (dotted line).

The model's response is close to the experimental curve in the first ascending branch and at large strains ($\varepsilon_0 > 0,3$). Instead of a horizontal plateau, the experimental curve exhibits a branch with variable positive slope. This discrepancy has already been the object of investigation [Puglisi and Truskinovsky (2001)], [Marzano et al. (2003)]. In particular, Puglisi and Truskinovsky reproduce the positive slope by considering a chain of springs with the same ascending branches, but separated by different barriers. Finally, Figure 6 shows the experimental curve at unloading [Pampolini (2007)]. It confirms the presence of the hysteresis loop predicted by the proposed model.

Table 1 Values of the constitutive constants.

	Material Constants
α	2.92 kPa
μ	2.92 kPa
c	69.9 kPa
m	6
β	3.5 kPa
k	18
a	0.72

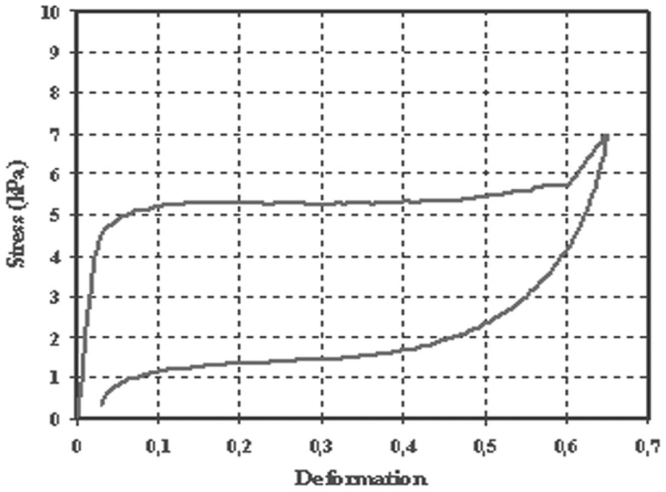

Fig. 6 Experimental response with hysteresis loop [Pampolini (2007)].

Acknowledgements This work was supported by the PRIN 2005 "Modelli Matematici per la Scienza dei Materiali" of the Italian Ministry for University and Research.

References

[Bardenhagen et al. (2005)] S. G. Bardenhagen, A. D. Brydon, and J. E. Guilkey. Insight into the physics of foam densification via numerical simulation. *J. Mech. Phys. Solids*, 53: 597–617, 2005.

[Bart-Smith et al. (1998)] H. Bart-Smith, A.-F. Bastawros, D. R. Mumm, A. G. Evans, D. J. Sypeck, and H. N. G. Wadley. Compressive deformation and yielding mechanisms in cellular al alloys determined using x-ray tomography and surface strain mapping. *Acta Materialia*, 46:3583–3592, 1998.

[Bastawros et al. (2000)] A.-F. Bastawros, H. Bart-Smith, and A. G. Evans. Experimental analysis of deformation mechanism in a closed-cell aluminium alloy. *J. Mech. Phys. Solids*, 48:301–322, 2000.

[Del Piero and Truskinowsky (2008)] G. Del Piero and L. Truskinowsky. Elastic bars with decohesions. *In preparation*, 2008.

[Gent and Thomas (1963)] A. N. Gent and A. G. Thomas. Mechanics of foamed elastic materials. *Rubber Chem. Technol*, 36:597–610, 1963.

[Gibson and Ashby (1997)] L. J. Gibson and M. F. Ashby. *Cellular Solids: Structure and Properties*. Cambridge University Press, second edition, 1997.

[Gioia et al. (2001)] G. Gioia, Y. Wang, and A. M. Cuitino. The energetics of heterogeneous deformation in open-cell solid foams. *Proc. R. Soc. London A*, 457:1079–1096, 2001.

[Gong and Kyriakides (2005)] L. Gong and S. Kyriakides. Compressive response of open-cell foams. part ii: Initiation and evolution of crushing. *Int. J. Solids Struct.*, 42:1381–1399, 2005.

[Gong et al. (2005)] L. Gong, S. Kyriakides, and W. Y. Jang. Compressive response of open-cell foams. part i: Morphology and elastic properties. *Int. J. Solids Struct.*, 42:1355–1379, 2005.

[Lakes et al. (1993)] R. Lakes, P. Rosakis, and A. Ruina. Microbuckling instability in elastomeric cellular solids. *J.Mater.Sci.*, 28:4667–4672, 1993.

[Marzano et al. (2003)] S. Marzano, M. D. Piccioni, and G. Puglisi. Un modello di isteresi per fili di leghe a memoria di forma. *Proc. 16th AIMETA National Congress of Theoretical and Applied Mechanics.*, 2003.

[Ogden (1997)] R.W. Ogden. *Non-Linear Elastic Deformations.* Dover Publications, New York, 1997.

[Pampolini (2007)] G. Pampolini. Experimental tests and theoretical model for strain localization and cyclic damage of polyurethane foam cylinders in uniaxial compression. *Communication at the VI Meeting Unilateral Problems in Structural Analysis, Siracusa*, 2007.

[Pampolini and Del Piero (2008)] G. Pampolini and G. Del Piero. Strain localization in polyurethane foams. Experiments and theoretical model. *in preparation*, 2008.

[Puglisi and Truskinovsky (2000)] G. Puglisi and L. Truskinovsky. Mechanics of a discrete chain with bi-stable elements. *J. Mech. Phys. Solids*, 48:1–27, 2000.

[Puglisi and Truskinovsky (2001)] G. Puglisi and L. Truskinovsky. Hardening and hysteresis in transformational plasticity. *Proc. 15th AIMETA National Congress of Theoretical and Applied Mechanics*, 2001.

[Wang and Cuitinho (2002)] Y. Wang and Y. Cuitinho. Full-field measurements of heterogeneous deformation patterns on polymeric foams using digital image correlation. *Int. J. Solids Struct.*, 39:3777–3796, 2002.

[Warren and Kraynik (1997)] W. E. Warren and A. M. Kraynik. Linear elastic behavior of a low-density kelvin foam with open cells. *ASME J. Appl. Mech.*, 64:787–793, 1997.